Estimation of Groundwater Recharge to the Aquifer Surrounding Buzwagi Gold Mine by Water Balance Method, in Northern Tanzania

Edwin Sifuel Gomezulu

St John's University of Tanzania, P.O.BOX 47 Dodoma, Tanzania

DOI: https://doi.org/10.51244/IJRSI.2026.1311000078

Received: 04 November 2026; Accepted: 09 November 2026; Published: 24 November 2026

ABSTRACT

Groundwater is an important source of water for domestic use, agriculture and mining activities in northwestern Tanzania. In the area surrounding Buzwagi Gold Mine (BGM), increasing water demand and mining-related activities highlight the need for reliable information on groundwater replenishment to support sustainable water-resource management and planning. Estimating groundwater recharge is essential because recharge represents the amount of water that replenishes the aquifer and helps assess the long-term availability of groundwater. This study aimed to estimate groundwater recharge in the aquifer surrounding Buzwagi Gold Mine using the water-balance method. A water-budget model incorporating precipitation, surface runoff, actual evapotranspiration, and changes in soil-water storage was employed. Rainfall data covering 16 years (2005–2020) were obtained from the Tanzania Meteorological Authority (TMA), while Landsat 8 satellite images for 2018 and 2020 were acquired from the USGS Global Visualization Viewer (GloVis). The satellite images were processed using supervised classification in ArcMap to identify land-use and land-cover categories and determine the composite curve number, a key parameter for estimating surface runoff. The classified land-cover categories included vegetation, built-up areas, water bodies, and barren land, resulting in a composite curve number of 76. Potential evapotranspiration was estimated using the Thornthwaite method and used to calculate actual evapotranspiration. The results indicated that actual evapotranspiration ranged from 662 to 1,435 mm year^{-1}, while surface runoff ranged from 253 to 863 mm year^{-1}. Estimated annual groundwater recharge ranged from 240 to 400 mm year^{-1}, with a mean of approximately 319 mm year^{-1}. These findings provide preliminary, site-specific estimates of groundwater recharge that can inform groundwater-resource assessment, sustainable abstraction planning, and water management in the BGM area. A key limitation of this study is the reliance on the water-balance method, which provides indirect estimates of groundwater recharge and may be affected by uncertainties in the estimation of precipitation, evapotranspiration, surface runoff, and soil-water storage.

Key words: Buzwagi gold mine, Curve number, Evapotranspiration, Groundwater, Recharge, Water balance.

INTRODUCTION

Groundwater recharge is defined as component of infiltration into the subsurface that joins groundwater through the unsaturated zone, the river bed or lake ground (Seiler and Gat, 2007). It is defined by Healy (2010) as the down flow of water reaching the water table adding to groundwater storage, it indicates the volume of water that can be extracted from an aquifer without depleting it. Groundwater recharge is a fundamental component of sustainable groundwater resource management and must be adequately considered in the planning, development, and management of groundwater resources (Veeranna and Jeet, 2020).

Groundwater recharge (GWR) is a critical component of sustainable groundwater resource management, particularly in regions where groundwater serves as the primary source of water for domestic, agricultural, and industrial uses. Its importance is especially pronounced in arid and semi-arid regions, where groundwater resources are often limited and replenishment rates are low, rendering many aquifers effectively non-renewable on human timescales (Crosbie *et al*., 2010; Margat *et al*., 2013). These areas experience minimal rainfall and high evaporation rates (Touham *et al*., 2014), leading to low recharge rates, found to be ranging

ISSN No. 2321-2705 | DOI: 10.51244/IJRSI |Volume XIII Issue XI November 2026

between 2% and 4% of the average annual precipitation in Iran (Jafari *et al*, 2019). Additionally, in arid regions, groundwater recharge is often lower than the combined effects of natural discharge and water withdrawals, creating an imbalance (Thomas *et al*., 2016).

Assessing recharge in mining areas is essential for efficient water management, as both local communities and mining operations rely on the same water source. Understanding groundwater recharge in such regions is fundamental for balancing groundwater withdrawals with natural replenishment. It provides the scientific basis for sustainable groundwater management, minimizes conflicts among competing water users, safeguards water quality against mining-related contamination, and ensures the long-term availability of groundwater for both mining operations and surrounding communities.

Several factors influence groundwater recharge, including soil type, bedrock characteristics, and the amount of available water in the water table. Additionally, land use and land cover changes have been identified as key factors affecting recharge rates (Mohan *et al*., 2018). Studies demonstrates that groundwater recharge varies with land cover because different LULC types modify infiltration, runoff, interception, and evapotranspiration (Owuor *et al*, 2016, Mengistu *et al*, 2022).

The rate at which water infiltrates the soil and moves into both unsaturated and saturated zones depends on soil properties. Soils are classified based on their infiltration capacity into four hydrological soil groups (HSG); A, B, C, and D. HSG A has the highest infiltration rate, exceeding 0.3 inches per hour, resulting in minimal runoff (Westenbroek *et al*., 2018). HSG B has a moderate infiltration rate, ranging from 0.15 to 0.3 inches per hour, and generates moderate runoff (Westenbroek *et al*., 2018). HSG C exhibits a lower infiltration rate between 0.05 and 0.15 inches per hour (Westenbroek *et al*., 2018). Lastly, HSG D, which consists of fine-textured soils, has a very low infiltration rate (below 0.05 inches per hour), leading to high runoff potential (Hawkins *et al*., 2009).

Hydrologic condition refers to how runoff and infiltration rates are influenced by land cover type and treatment. Cover types include vegetation, bare soil, and impervious surfaces, while treatment describes the modifications made to the land cover. These modifications may include practices such as contouring, terracing, crop rotation, and tillage (Ahuchaogu *et al*, 2022). There are three classifications of hydrologic condition: good, fair, and poor (Yoon *et al*, 2025). A good hydrologic condition is associated with low runoff potential, whereas a poor condition corresponds to high runoff potential. For this study, the hydrologic condition of the area was assumed to be fair. There are several techniques available for estimating groundwater recharge (GWR), including chloride mass balance, Darcy's Law, Soil Water Balance, Water Table Fluctuation (WTF), and the Water Balance Method, among others (Scanlon et *al*, 2002; Healy, 2010). This study specifically uses the Water Balance Method to estimate GWR.

The Water Balance which is also called Water Budget is an accounting of water movement into and out of, and storage change within, some control volume (Healy, 2010). It was originally developed by Thornthwaite in 1948 and subsequently modified by various researchers over the years (Kumar, 2021). The water balance method (WBM) is widely applied for groundwater recharge estimation because it utilizes readily available hydrological and meteorological data and is underpinned by a robust, well-established conceptual framework (Healy, 2010). Despite the presence of the Buzwagi Mine and its long-standing, high demand for groundwater resources, research on groundwater recharge in the study area remains limited. This study therefore aims to fill this knowledge gap by estimating groundwater recharge within the study area.

METHODS

The study area

The study area is located in north-western Tanzania, within Shinyanga Region, in an area surrounding Buzwagi Gold Mine (BGM). The area is selected for this study because of its high dependence on groundwater, which serves as the primary source of water for domestic, agricultural, and mining activities. The area also hosts intensive gold mining operations, which exert considerable pressure on the available

ISSN No. 2321-2705 | DOI: 10.51244/IJRSI |Volume XIII Issue XI November 2026

groundwater resources. Shinyanga Region lies between latitudes 2° 9′ 0″ and 2° 21′ 36″ S and longitudes 35° 13′ 12″ and 31° 11′ 24″ E (Fig.1)

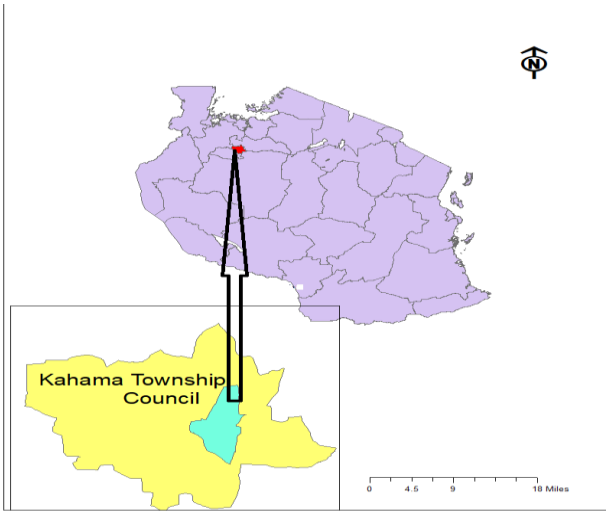


Figure 1. The map of Tanzania showing the study area

The region experiences a tropical savanna climate characterized by warm temperatures throughout the year, typically ranging from 25°C to 32°C. The area has distinct wet and dry seasons, with warm daytime conditions, relatively cooler evenings, and noticeable winds, particularly during August.

Geological Setting of the Study Area

The area contains seven main geological formations; **K-feldspar Granite** or **K-rich Granite (**KFGT), **Na-rich Granite** or sodic granite (NAGT), Tonalite (TNL), Quartz Sericite Granite (QSGT), SHGT, **Mafic Volcanic** (MVOL), and Ultramafic Rocks (UMAF) (Figure 2)

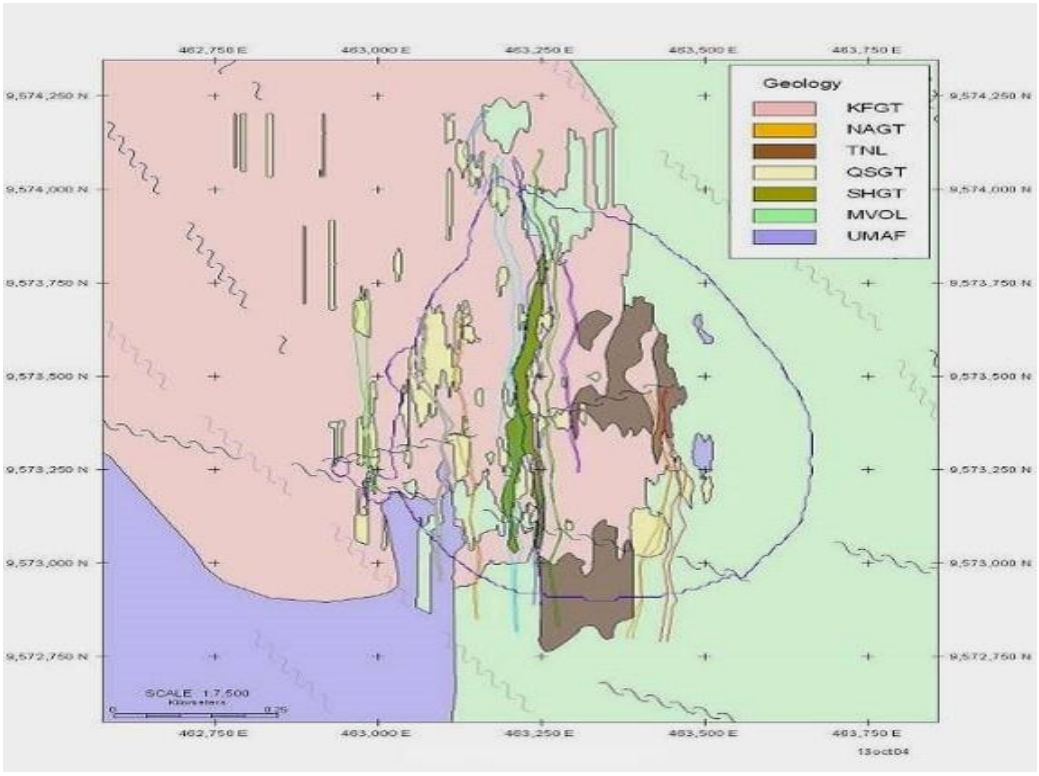


Figure 2. Geological formation of the study area (Source: Geological survey of Tanzania)

The dominant rock unit is KFGT, which occupies most of the western and central regions. This distribution suggests that KFGT represents the regional basement complex or the most extensive lithological unit within

the area. The eastern part of the area is predominantly underlain by MVOL, indicating the presence of volcanic rocks that constitute a broad eastern geological domain. In the southwestern corner UMAF occurs as a distinct unit, likely representing ultramafic rocks or intrusive bodies. TNL occurs as irregular bodies in the central and southern sections of the map. These may represent intrusive rocks or metamorphosed sedimentary units associated with structural zones. NAGT occurs in small isolated patches, likely representing minor intrusive or altered zones. QSGT and SHGT occur as narrow, elongated bodies trending predominantly North South. Their linear nature suggests they may follow shear zones, fractures, or lithological contacts.

Since KFGT unit covers most of the area they likely represent crystalline basement rocks such as granites or gneisses. Because this unit is widespread, groundwater recharge in the area depends heavily on the intensity of weathering and fracturing within the KFGT rocks. Areas with dense fractures or deep weathering have better recharge and groundwater storage. According to Ahrens *et al*, (2018), Tonalite has a structure which resists groundwater flow as compared to K granite. The mafic volcanic units represent volcanic or metavolcanic rocks. Their influence on groundwater recharge depends largely on the extent of fracturing and weathering. Highly fractured, porous, or weathered volcanic rocks can enhance groundwater recharge by increasing permeability, whereas compact and unfractured volcanic rocks may restrict recharge due to their low permeability.

The UMAF unit occurs in the southwestern part of the study area as a relatively limited geological body. Ultramafic rocks are typically composed of dense ferromagnesian minerals such as olivine and pyroxene, which form tightly interlocking crystalline textures with very little primary pore space (Brooks, 2024). Consequently, these rocks generally exhibit very low porosity and permeability unless extensively fractured. In addition, ultramafic rocks often weather to form thin, clay-rich regolith layers that can impede the infiltration and movement of groundwater. The limited aerial extent of the UMAF unit on the geological map further suggests a restricted contribution to groundwater storage and recharge compared to the more extensive surrounding lithological units (Pradhan *et al*, 2022). These rocks typically produce thin soils and high surface runoff and therefore reduce infiltration. As a result, groundwater recharge is likely low in UMAF areas except where intense fracturing occurs. Permeability of UMAF have shown to be greater than MVOL (Bayrakci *et al*, 2018).

The SHGT and QSGT on the geological map (Figure 2), appear as narrow, elongated and linear rock bodies. Their shape suggests that they occur along zones of weakness in the rocks, such as fractures, faults and shear zones. These structural zones are important pathways for groundwater movement.

The TNL, SHGT, QSGT, and NAGT rock units are shaped and positioned along fractured and faulted zones. These broken rock zones allow rainwater to enter and move underground more easily, making them important areas for groundwater recharge and groundwater flow.

Data collection

Two main types of data were used in this study; meteorological data and satellite imagery. The meteorological data, comprising monthly precipitation records, were obtained from the Tanzania Meteorological Authority (TMA). The dataset comprises 16 years of monthly rainfall records covering the period 2005 to 2020. Satellite imagery for the years 2018 and 2020, acquired by Landsat 8, was obtained from the United States Geological Survey (USGS) through the Global Visualization Viewer (GloVis) platform. The satellite scenes were identified and acquired according to the Landsat Worldwide Reference System (WRS), with the study area falling within Path 060 and Row 170 (WRS Path/Row 060/170). This path and row combination was used to identify and acquire the Landsat scenes covering the study area for subsequent image processing and analysis.

The acquired Landsat images were clipped to the study-area boundary using the **Extract by Mask** tool in ArcMap. The images were then classified to determine the major land-cover characteristics of the study area. The resulting land-cover information, together with soil characteristics and hydrologic conditions, was used to assign the appropriate curve number (CN). The CN is a key parameter in the estimation of surface runoff using the Soil Conservation Service Curve Number (SCS-CN) method. The estimated runoff was subsequently incorporated into the water-budget model for estimating groundwater recharge.

ISSN No. 2321-2705 | DOI: 10.51244/IJRSI |Volume XIII Issue XI November 2026

Determination of recharge

In the water-balance model, groundwater recharge is estimated using the water-budget equation presented by Soltani *et al.* (2020), as shown in Equation (1). The method was chosen because it is a simple and practical approach that quantifies the major components of the hydrological cycle, including total water losses from the soil through evapotranspiration and runoff (Wilson *et al*, 2001). In addition, the model relies on commonly available climatic and hydrological data, making it suitable for areas where detailed hydrogeological data are limited

$R_i = P - E_a + \Delta W - R_o$, ……(1)

where R_i= recharge, E_a= Actual Evapotranspiration, P= precipitation, ΔW= change in soil water storage and Ro= runoff. The value of R_o is estimated by the run off equation given by:

$Ro = \left(\frac{(P-0.2S)^2}{P+0.8S}\right)$ ……(2)

where P= Precipitation (in mm), R_o=runoff (in mm) and S is the Potential maximum retention after runoff begins and it is given by: $S = \frac{1000}{CN} - 10$ (SCS,1986) ……(3)

where CN= runoff curve number. Curve number is related to soil texture, soil infiltration capability and the land cover (Ahmad- Sani *et al*, 2022).

Change in storage (ΔW) is calculated by Thorn Thwaite–Mather water balance (equation 4)

$\Delta W = S_i - S_{i-1}$ …… (4)

Where ΔS = change in soil water storage (mm), S_i = soil moisture storage in the current month (mm) and S_{i-1} = soil moisture storage in the previous month (mm).

The Potential maximum retention after runoff begins (S) is related to initial abstraction (Ia) by the equation Ia= 0.2S……(5)

Estimation of Actual Evapotranspiration (AET)

The Actual evapotranspiration (AET) was calculated from potential evapotranspiration (PET). PET is calculated by using Thornthwaite method. According to Thornthwaite method, PET is calculated by the formula as in equation 6.

$PET = 1.6b\left(\frac{10Ta}{I}\right)^a$ ……(6)

where I = annual heat index (a measure that combines **air temperature** and **relative humidity**), which is given by

$\sum i_m$ whereby $i_m = \sum\left(\frac{Tm}{5}\right)^{1.5}$ ……(7)

Tm= average monthly temperature b= monthly correction factor for latitude effect; the value which depends on geographical location and Ta= monthly mean temperature (^{0}C). According to Thornthwaite, a is calculated from annual heat index (I) by using the formula in equation 8.

$a = 6.7 \times 10^{-7}I^3 - 7.7 \times 10^{-5}I^2 + 1.8 \times 10^{-2}I + 0.49.$ ……(8)

Actual evapotranspiration (AET) is considered to be equal to potential evapotranspiration (PET) when P-PET>0 and AET= |ΔSM|+ P-PET, when P-PET<0.

Sensitivity Analysis

One-at-a-Time (OAT) approach as outlined by Saraiva *et al,* (2017) was used in Sensitivity analysis (SA). In this method each input parameter is varied individually while all other parameters are maintained at their baseline values. This approach enables the relative contribution of each parameter to the variability in groundwater recharge estimates to be quantified. The SA considers the principal input variables used in the recharge estimation, namely precipitation (P), mean air temperature (Ta), curve number (CN), and change in soil water storage (ΔW). In this method each parameter is independently changed by ±10% and ±20% from its baseline value while the remaining parameters are held constant. Recharge is then recalculated for each change, and the corresponding percentage change in recharge is determined using the equation 9.

$$\%\Delta R_i = \frac{R_{i,new} - R_{i,base}}{R_{i,base}} \times 100 \quad \text{.....(9)}$$

where $R_{,i,\ base}$ is the recharge estimated using the baseline parameter values and $R_{i,\ new}$ is the recharge estimate obtained after modifying one model input parameter, with all other parameters held constant. In order to quantify the relative influence of each parameter, a normalized sensitivity index (SI) is calculated as given by Saraiva *et al,* (2017) as shown by equation 10.

$$SI = \frac{\Delta R_i / R_i}{\Delta X / X} \quad \text{.....(10)}$$

where x represents the modified input parameter, Δx is the imposed change in the parameter, R_i is the baseline recharge, and ΔR_i is the corresponding change in recharge.

If |SI|>1 it indicates high sensitivity, and if 0.5≤|SI|≤10.5 it indicates moderate sensitivity, and if |SI|<0.5|SI|<0.5|SI|<0.5 it indicates low sensitivity.

RESULTS AND DISCUSSION

Soil characteristics play a critical role in determining runoff because they control infiltration, storage, and movement of water within the soil profile. Studies demonstrate that the predominant soil type in the study area is **Phaeozems (MARI, 2006,** Nachtergaele *et al*, 2010**);** these soils are porous, fertile, and contain 10 to 20% clay. They are characterized by their dark color and high humus content. As noted by Labaz *et al* (2024), soils similar to Phaeozems are typically black and rich in organic matter. They are generally well-drained due to their good structure and porosity. The HSG for the soil in the study area falls under HSG B.

Determination of a Runoff Curve Number (CN)

The runoff curve number (CN) is influenced by factors such as hydrologic soil group, land-cover type, land treatment, and hydrologic condition (Sreejith *et al*., 2024). A higher CN value indicates greater surface runoff. According to Ahmad-Sani *et al.* (2022), the CN is also associated with soil texture, soil infiltration capacity, land use, and the depth of the seasonal high water table. To estimate the composite CN for the study area, a weighted average of the curve numbers assigned to the different land-cover types was calculated based on their respective proportions of the total area. The 2018 and 2020 Satellite images were classified using supervised classification in ArcMap. The CN was determined for each classified image, and the overall CN for the study area was calculated as the mean of the values obtained for the two years. The classified 2018 image (Figure 3) shows the percentage distribution of the different land-cover types. Vegetation was the dominant land-cover type, occupying the largest proportion of the study area, whereas water bodies occupied the smallest proportion, as detailed in Table 1.

Table 1. Areas and percentage areas of different cover types in areas surrounding BGM in 2018

Cover type	Area (Ha)	% area
Vegetation	5519	57.6

ISSN No. 2321-2705 | DOI: 10.51244/IJRSI |Volume XIII Issue XI November 2026

Built up area	2797	29.2
Barren land	944	9.85
Water body	319	3.35

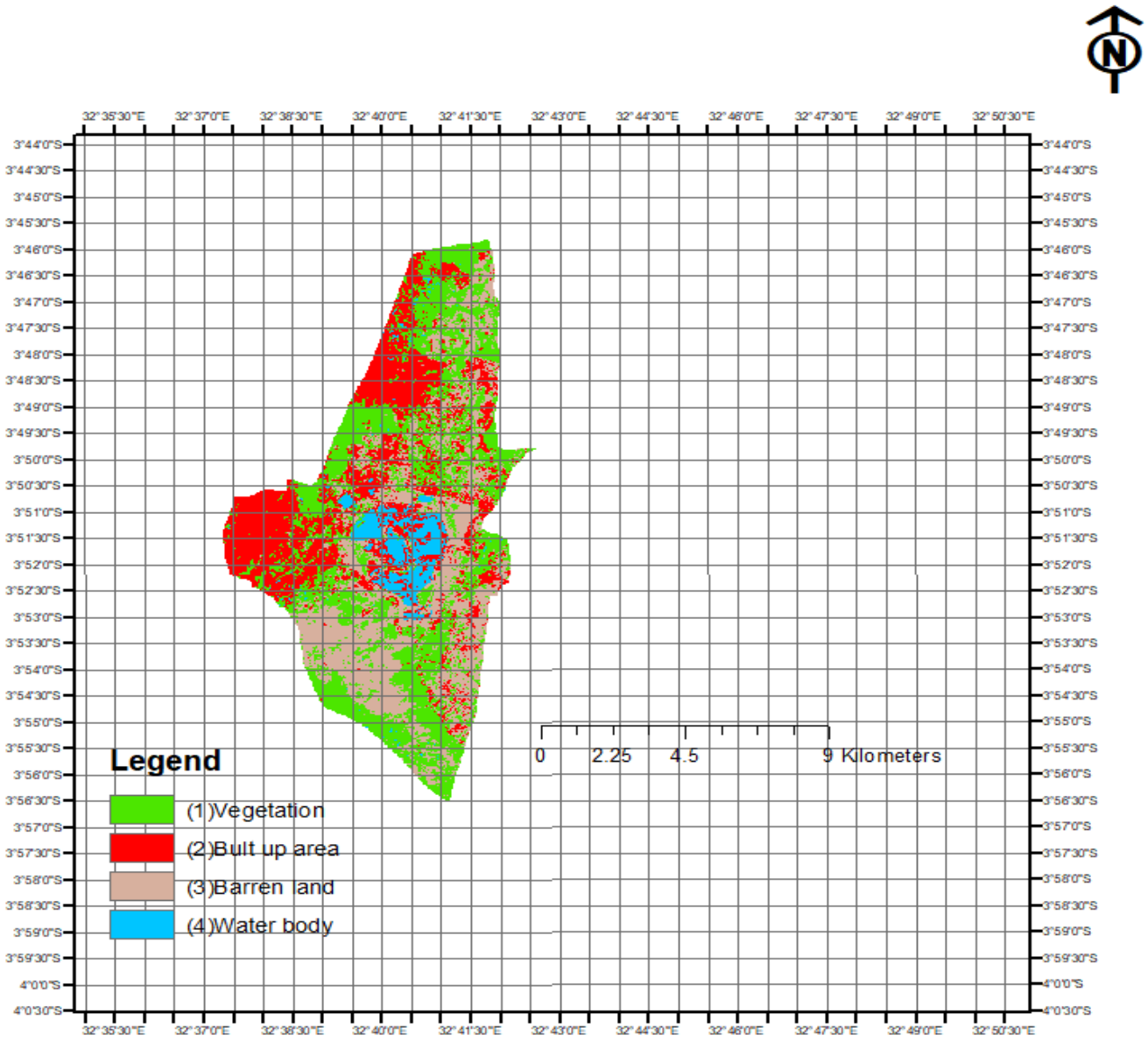


Figure 3. The Classified satellite image of 2018 in areas surrounding BGM

The classified 2020 image (Figure 4) shows the percentage distribution of the different land-cover types, as presented in Table 2. Vegetation was the dominant land-cover type, occupying the largest proportion of the study area, whereas water bodies occupied the smallest proportion.

Table 2. Areas and percentage areas of different cover types in area surrounding BGM in 2020

Cover type	Area (hectares)	% cover
Vegetation	3686	38.2
Water body	413	4.28
Built up area	3406	35.3
Barren land	2144	22.22

ISSN No. 2321-2705 | DOI: 10.51244/IJRSI |Volume XIII Issue XI November 2026

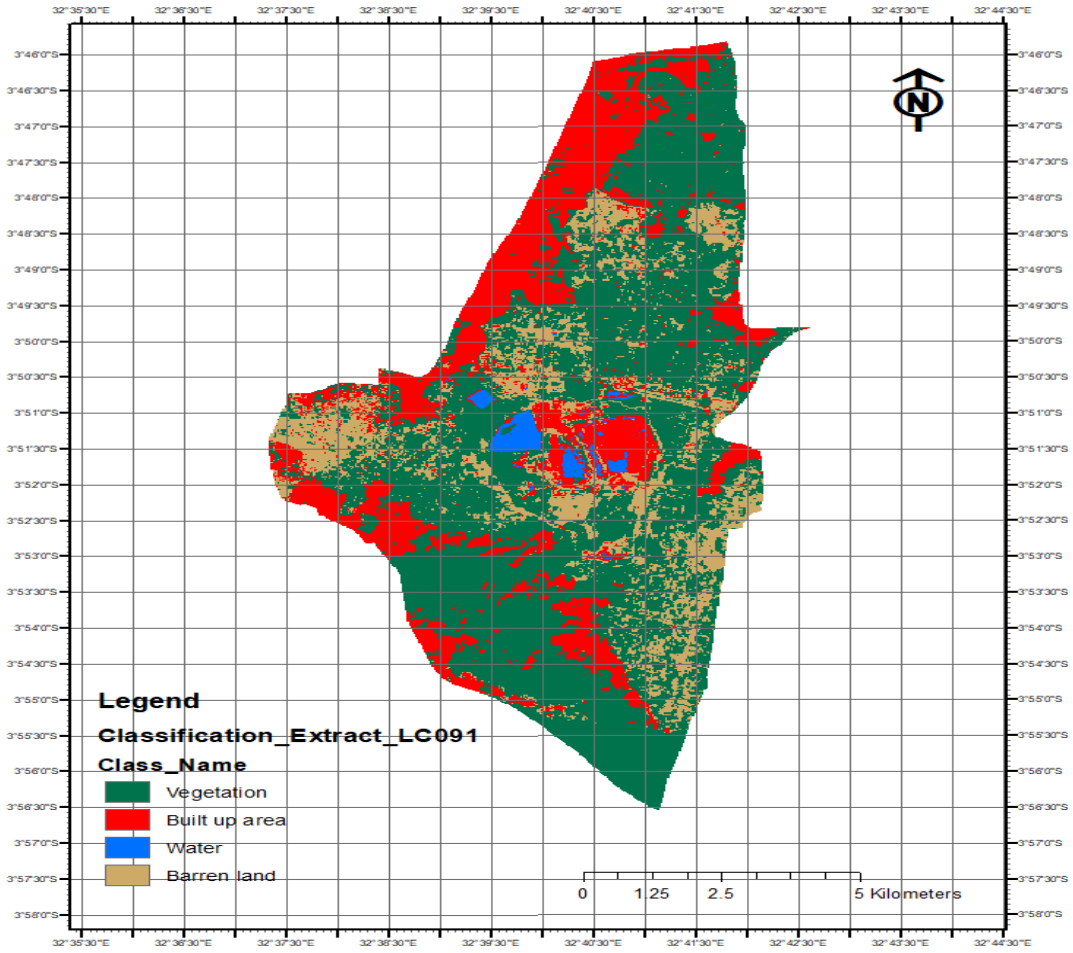


Figure 4. The classified satellite image of 2020 in areas surrounding BGM

The curve number (CN) was determined using land-cover data derived from Moderate Resolution Imaging Spectroradiometer (MODIS) imagery and the corresponding CN values assigned to different land-cover types under fair hydrologic conditions, as presented in Table 3. These values were used to calculate the composite CN for the study area. The resulting composite CN was then used to estimate surface runoff, an important component of the water-budget approach for estimating groundwater recharge.

Table 3. CN derived from MODIS land cover classification and hydrological soil groups (HSGs) under fair hydrological conditions

	MODIS land cover classification	CN for different HSG				
ID	Content	A	B	C	D	Hydrological condition
0	Water bodies	N/A	N/A	N/A	N/A	N/A
1	Evergreen needles	34	60	73	79	Fair
2	evergreen broadleaf	30	58	71	77	Fair
3	Deciduous needle leaf	40	64	77	83	Fair
4	Deciduous broadleaf	42	66	79	85	Fair
5	Mixed forests	38	62	75	81	Fair
6	Closed shrublands	45	65	75	80	Fair
7	Open shrublands	49	69	79	84	Fair

8	Woody savannas	61	71	81	89	Fair
9	Savannas	72	80	87	93	Fair
10	Grasslands	49	69	79	84	Fair
11	Permanent wetlands	30	58	71	78	Fair
12	Croplands	52	69	79	84	Fair
13	Urban and built-up	80	85	90	95	Fair
14	Cropland/Natural vegetation mosaic	80	85	90	95	Fair
15	Permanent snow and ice	N/A	N/A	N/A	N/A	Fair
16	Barren or sparsely vegetated	72	82	83	87	Fair
17	Missing data	N/A	N/A	N/A	N/A	Fair

(Source: Modified from USDA (1986) and NEH-4 (1997) lookup tables)

The CNc can thus be derived from the MODIS by the formula:

$$CN_C = \frac{\sum(CN_i \times A_i)}{\sum A_i} \quad \text{.....(11)}$$

A_i = area of the land cover for soil group combination i. CN_i = curve number for combination i (based on land cover class and HSG under fair conditions) and $\sum A_i$ = total area considered (sum of all individual areas). The land covers obtained for the present study are represented in figures 3 and 4, while the corresponding areas are provided in tables 1 and 2. The CNc was calculated separately for each year, and the mean of the two annual values was used as the representative curve number for the study area. The resulting composite curve number was 76.

Variability of Rainfall, Actual Evapotranspiration and Runoff

Figure 5 illustrates the temporal variation in the major hydrological components; precipitation, Actual Evapotranspiration, surface runoff, and groundwater recharge in the area surrounding BGM between 2005 and 2020. These components exhibit pronounced interannual variability and strong hydrological interdependence, reflecting the influence of climatic variability on the groundwater system.

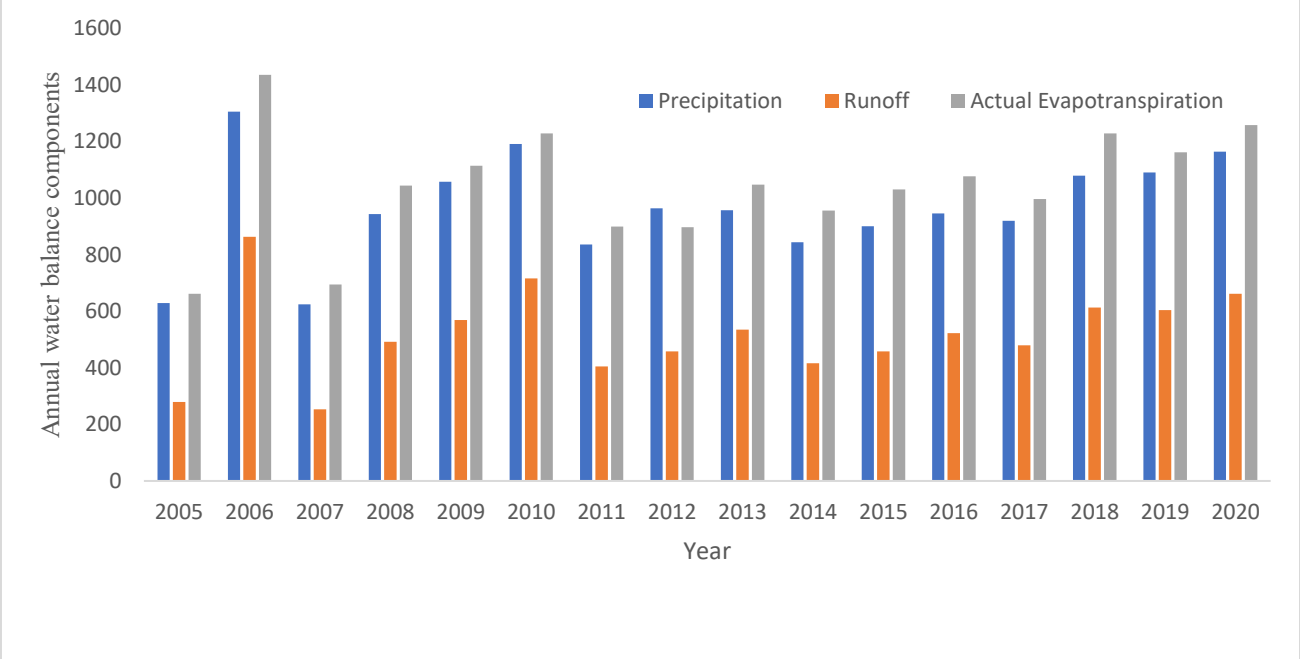


Figure 5. Precipitation, runoff and Actual Evapotranspiration in area surrounding BGM

Annual precipitation ranges from a minimum of 629 mm year^{-1} in 2005 to a maximum of approximately 1,305 mm year^{-1} in 2006, with a long-term mean of 965.4 mm year^{-1}. This represents a difference of about 676 mm year^{-1} between the driest and wettest years, indicating considerable variability in rainfall over the study period. Although annual rainfall fluctuates substantially from year to year, an overall increasing tendency was observed during the periods 2007–2010 and 2014–2020, suggesting a gradual increase in precipitation in

recent years. Such variations are likely associated with natural climate variability, including changes in the intensity and distribution of seasonal rainfall. An average annual rainfall of approximately 965 mm year^{-1} may be regarded as moderate for the semi-humid tropical conditions of northwestern Tanzania. However, the wide interannual fluctuations indicate that water availability is highly variable, with some years receiving substantially less rainfall than the long-term average. The years with rainfall below 700 mm year^{-1} are likely to experience limited groundwater replenishment because a greater proportion of the available precipitation is consumed by evapotranspiration and soil moisture replenishment before deep percolation can occur. Conversely, the years receiving rainfall above 1,200 mm year^{-1} are expected to generate greater runoff and increased groundwater recharge once the soil water storage capacity has been satisfied. The observed rainfall variability has important implications for groundwater availability in the BGM area, where groundwater constitutes the principal source of water for domestic consumption, mining operations, and other socioeconomic activities. Sustained periods of below average rainfall may reduce recharge and lower groundwater levels, whereas wetter years contribute significantly to aquifer replenishment. Therefore, understanding the temporal variability of precipitation is essential for evaluating groundwater recharge and developing sustainable groundwater management strategies capable of supporting the increasing water demand associated with long-term mining activities.

Actual evapotranspiration (AET) closely followed the temporal pattern of precipitation, reflecting the strong influence of climatic conditions on atmospheric water loss. AET varied from approximately 662 mm year^{-1} in 2005 to about 1,435 mm year^{-1} in 2006, indicating considerable interannual variability. The higher AET observed during 2006 and throughout the periods 2007–2010 and 2012–2020 coincided with years of relatively high rainfall, suggesting that increased water availability enhanced evapotranspiration. Under such conditions, greater soil moisture and increased vegetation activity provide sufficient water for evaporation and transpiration, resulting in higher AET rates. Conversely, the relatively low AET recorded in 2005 is consistent with below-average rainfall, when limited soil moisture availability restricts evapotranspiration. The magnitude of annual AET is relatively high, with values exceeding annual precipitation in some years. This suggests that evapotranspiration constitutes the largest component of the water balance and represents a major pathway of water loss from the catchment. Such high evaporative demand limits the proportion of rainfall available for surface runoff and groundwater recharge, particularly during years of low precipitation. Consequently, groundwater replenishment is likely to be highly sensitive to changes in rainfall amount and distribution.

Annual runoff ranges from approximately 253 to 863 mm year^{-1}, with the maximum occurring in 2006 and the minimum in 2007. The exceptionally high runoff in 2006 corresponds to the wettest year of the study period, indicating that rainfall exceeded the infiltration and storage capacity of the soil, thereby generating greater surface flow. In contrast, lower runoff during relatively dry years reflects reduced rainfall inputs and diminished surface water generation. Overall, runoff exhibited an increasing tendency over the study period, although interannual fluctuations were evident, particularly in 2014 and 2017, reflecting the influence of rainfall variability and catchment hydrological responses. The strong positive correlation between precipitation and runoff ($r = 0.90$) demonstrates that rainfall is the primary driver of runoff generation in the study area, it also indicates that the catchment responds rapidly to rainfall events, with limited capacity to retain water through soil storage and infiltration. As a result, increases in rainfall are quickly reflected in higher surface runoff. From a groundwater perspective, the years characterized by high runoff may not necessarily produce proportionally high groundwater recharge, as a substantial fraction of rainfall is exported as surface flow rather than infiltrating into the subsurface. Therefore, evaluating runoff alongside evapotranspiration and recharge is essential for understanding the partitioning of rainfall and for developing sustainable groundwater management strategies in the BGM area, where groundwater is the principal source of water for domestic use and mining operations.

ISSN No. 2321-2705 | DOI: 10.51244/IJRSI |Volume XIII Issue XI November 2026

Groundwater recharge

Groundwater recharge in the Buzwagi Gold Mine (BGM) area increased from approximately 240 mm year^{-1} in 2005 to 400 mm year^{-1} in 2020, indicating an overall upward trend in estimated annual recharge during the study period (Figure 6).

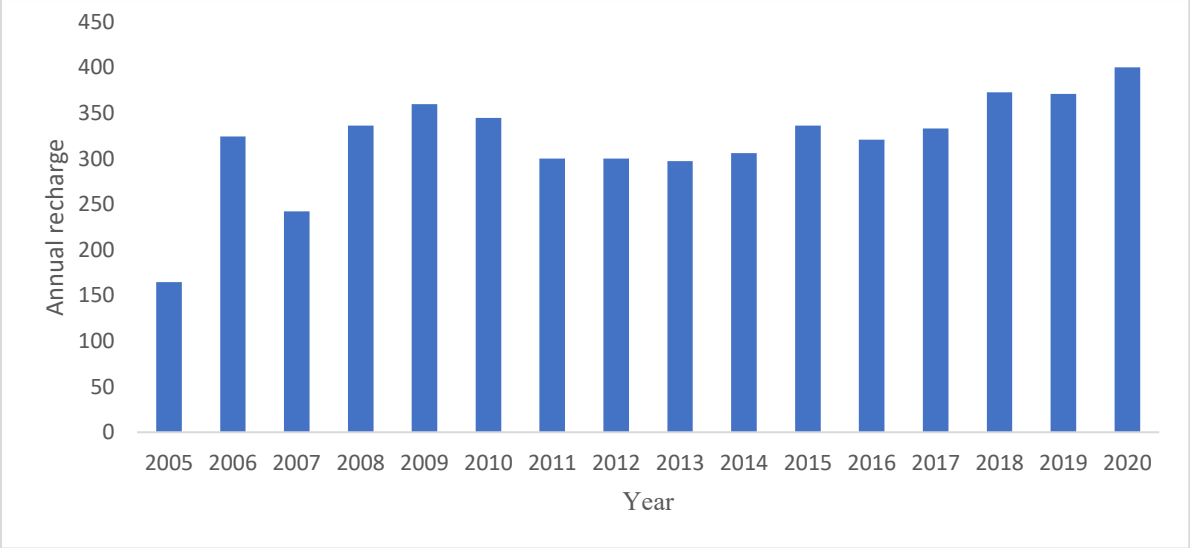


Figure 6. Annual Groundwater Recharge, Buzwagi Gold Mine (2005-2020)

Despite some interannual fluctuations, the results suggest an increase in the amount of water potentially available for aquifer replenishment. The estimated mean recharge of 319.4 mm year^{-1} indicates that groundwater recharge represents an important component of the local water balance. However, the increasing recharge trend does not necessarily demonstrate a corresponding increase in groundwater storage or availability, as these also depend on groundwater abstraction, subsurface discharge, and changes in aquifer storage.

Compared with estimates reported in other regions, the mean recharge in the BGM area is relatively high. Previous studies reported an average of 148 mm year^{-1} in Arusha, Tanzania (Kiflay *et al*., 2025), 235.15 mm year^{-1} in Burundi (Bakundukize *et al*., 2011), recharge estimates of 250.1–269.2 mm year^{-1} under different seasonal conditions in Mbeya, Tanzania (Sahinkuye *et al*., 2025), and an average of 256.2 mm year^{-1} in Dar es Salaam, Tanzania (Mjemah *et al*., 2010). Although these comparisons suggest relatively high recharge in the BGM area, differences in climatic conditions, geological settings, land cover, estimation periods, and methodological approaches may contribute to the variation among study areas. Therefore, the differences should not be attributed solely to more favorable recharge conditions in the BGM area.

The spatial and temporal variability in groundwater recharge can be explained partly by the interaction between rainfall, evapotranspiration, runoff, soil properties, land cover, and geological characteristics. Precipitation supplies water for both surface and subsurface processes, while evapotranspiration reduces the amount of water remaining for recharge. Runoff further influences the proportion of rainfall available for infiltration. In the BGM area, the predominance of K-rich feldspar granite in the western and central parts, together with volcanic formations and other geological units, may influence groundwater movement and storage through variations in weathering, fracturing, and permeability. Fractures, faults, and shear zones may provide preferential pathways for infiltration where they are sufficiently open and hydraulically connected. Similarly, soil properties and changes in land cover may affect infiltration capacity and the partitioning of rainfall among runoff, evapotranspiration, and subsurface recharge.

The annual variations in precipitation, runoff, and actual evapotranspiration provide further context for interpreting the recharge estimates. However, increased precipitation does not necessarily result in a proportional increase in groundwater recharge as additional rainfall may also contribute to increased surface runoff and evapotranspiration. Consequently, the observed recharge pattern reflects the combined effects of

climatic variability and land-surface and subsurface processes represented in the water-balance model. Changes in vegetation and built-up areas during the study period may also have influenced infiltration and runoff partitioning, although their individual contributions cannot be quantified from the recharge estimates alone.

These findings provide a useful baseline for groundwater resource assessment and management in the BGM area, where groundwater is important for domestic, agricultural, and mining activities. The estimated recharge values can support preliminary assessments of groundwater replenishment and inform decisions on monitoring and resource protection. Nevertheless, the water-balance method is subject to uncertainty associated with rainfall records, evapotranspiration estimates, runoff curve-number selection, soil-moisture accounting, and assumptions concerning the representation of local hydrogeological conditions. Future research should therefore integrate the water-balance estimates with groundwater-level monitoring, aquifer hydraulic-property measurements, and independent recharge-estimation methods to improve confidence in the results and establish whether the estimated recharge trend corresponds to changes in groundwater storage and long-term availability.

Sensitivity Analysis Results

Precipitation exhibits the highest sensitivity (1.25), followed by the curve number (CN) (0.92) and actual evapotranspiration (AET) (0.90), whereas soil water storage shows the lowest sensitivity (0.20). This ranking indicates that precipitation is the most influential parameter affecting groundwater recharge in the study area, although CN and AET also exert substantial influences. The high sensitivity of recharge to precipitation is attributable to the fact that precipitation represents the primary water input to the hydrological system. It directly contributes to groundwater recharge through the water-budget equation (Equation 1) and indirectly influences runoff generation and soil-water replenishment. The relatively low sensitivity of soil water storage (0.20) indicates that variations in soil water storage have a comparatively limited influence on the estimated long-term groundwater recharge.

CONCLUSION

This study estimated groundwater recharge in the aquifer surrounding the Buzwagi Gold Mine, in northwestern Tanzania, using a water balance approach that integrated precipitation, actual evapotranspiration (AET), surface runoff, and changes in soil water storage. Analysis of hydro-meteorological data from 2005 to 2020 showed considerable temporal variability, with annual precipitation ranging from 629 to 1,305 mm year^{-1}, AET from 662 to 1,435 mm year^{-1}, surface runoff from 253 to 863 mm year^{-1}, and groundwater recharge from 240 to 400 mm year^{-1}, yielding a mean annual recharge of approximately 319.4 mm year^{-1}. Sensitivity analysis identified precipitation as the dominant control on groundwater recharge (SI = 1.25), followed by the curve number (SI = 0.92) and AET (SI = 0.90), while soil water storage had relatively low influence (SI = 0.20).

The study demonstrates that integrating a water balance model with remotely sensed land-use information provides a practical and cost-effective approach for estimating groundwater recharge in data-limited mining regions. The findings provide valuable baseline information for groundwater allocation, sustainable abstraction planning, and long-term water resource management in the Buzwagi Gold Mine area.

The study is limited by the absence of field validation using independent recharge estimation techniques and by uncertainties associated with model assumptions and land-cover data. Future research should incorporate groundwater level monitoring, tracer- or isotope-based validation, higher-resolution remote sensing datasets, and climate change assessments to improve recharge estimation and support sustainable groundwater management.

REFERENCES

1. Ahmadi-Sani, N., Razaghnia, L., & Pukkala, T. (2022). *Effect of Land-Use Change on Runoff in Hyrcania. Land 2022, 11, 220.*

2. Ahuchaogu, I. (2022). Effects of Soil and Water Conservation Measures on the Environment-A Review. *Scientific Journal AGRICULTURAL ENGINEERING*.
3. Arnold, J. G., Muttiah, R. S., Srinivasan, R., & Allen, P. M. (2000). Regional estimation of base flow and groundwater recharge in the Upper Mississippi river basin. *Journal of hydrology*, *227*(1-4), 21-40.
4. Bakundukize, C., Van Camp, M., & Walraevens, K. (2011). Estimation of groundwater recharge in Bugesera region (Burundi) using soil moisture budget approach. *Geologica belgica*, *14*(1-2), 85-102.
5. Brooks, K. (2024). Peridotites and other ultramafic rocks. *Geology Today*, *40*(5), 201-207.
6. Crosbie, R. S., McCallum, J. L., Walker, G. R., & Chiew, F. H. (2010). Modelling climate-change impacts on groundwater recharge in the Murray-Darling Basin, Australia. *Hydrogeology Journal*, *18*(7), 1639-1656.
7. Hawkins, R. H., Ward, T. J., Woodward, D. E., & Van Mullem, J. A. (Eds.). (2008, November). Curve number hydrology: State of the practice. American Society of Civil Engineers.
8. Healy, R. W., & Scanlon, B. R. (2010). *Estimating groundwater recharge* (Vol. 245). Cambridge, MA: Cambridge university press.
9. Healy, R. W., & Scanlon, B. R. (2010). *Estimating groundwater recharge* (Vol. 245). Cambridge, MA: Cambridge university press.
10. Kumar, P. J. S., Schneider, M., & Elango, L. (2021). The state-of-the-art estimation of groundwater recharge and water balance with a special emphasis on India: A critical review. *Sustainability*, *14*(1), 1-16.
11. Labaz, B., Kowalska, J. B., Kabala, C., Kobierski, M., Waroszewski, J., Dudek, M., ... & Gruszka, D. (2024). Distribution and pools of soil organic carbon in chernozemic soils impacted by intensive farming and erosion in the loess plateau in south-east Poland. *Agronomy*, *14*(11), 2544.
12. Margat, J., & Van der Gun, J. (2013). *Groundwater around the world: a geographic synopsis*. Crc Press.
13. Mengistu, T. D., Chung, I. M., Kim, M. G., Chang, S. W., & Lee, J. E. (2022). Impacts and implications of land use land cover dynamics on groundwater recharge and surface runoff in East African Watershed. *Water*, *14*(13), 2068.
14. Mjemah, I. C., Van Camp, M., Martens, K., & Walraevens, K. (2011). Groundwater exploitation and recharge rate estimation of a quaternary sand aquifer in Dar-es-Salaam area, Tanzania. *Environmental Earth Sciences*, *63*(3), 559-569.
15. Mohan, C., Western, A. W., Wei, Y., & Saft, M. (2018). Predicting groundwater recharge for varying land cover and climate conditions–a global meta-study. *Hydrology and Earth System Sciences*, *22*(5), 2689-2703.
16. Nachtergaele, F., Van Velthuizen, H., Verelst, L., Batjes, N., Dijkshoorn, K., van Engelen, V., ... & Prieler, S. (2010, August). Harmonized world soil database. In *Proceedings of the 19th world congress of soil science, soil solutions for a changing world, Brisbane, Australia* (Vol. 2010, pp. 34-37). International Union of Soil Sciences.
17. Owuor, S. O., Butterbach-Bahl, K., Guzha, A. C., Rufino, M. C., Pelster, D. E., Díaz-Pinés, E., & Breuer, L. (2016). Groundwater recharge rates and surface runoff response to land use and land cover changes in semi-arid environments. *Ecological Processes*, *5*(1), 16.
18. Sahinkuye, T., Richard, S. F., Andrew, T., Japhet, K. J., & Winfred, M. (2025). Assessment of groundwater recharge variability in the Usangu Plains under projected climate scenarios (2021–2050) for RCP 4.5 and RCP 8.5. *Journal of Water and Climate Change*, *16*(10), 2867-2882.
19. Saraiva, J. P., Lima, B. S., Gomes, V. M., Flores, P. H., Gomes, F. A., Assis, A. O., ... & Calixto, W. P. (2017, May). Calculation of sensitivity index using one-at-a-time measures based on graphical analysis. In *2017 18th International Scientific Conference on Electric Power Engineering (EPE)* (pp. 1-6). IEEE.
20. Scanlon, B. R., Healy, R. W., & Cook, P. G. (2002). Choosing appropriate techniques for quantifying groundwater recharge. *Hydrogeology journal*, *10*(1), 18-39.
21. Sreejith, K. S., Kumar, G. P., & Dwarakish, G. S. (2024). A critical review of the soil conservation services–curve number method in hydrological modelling. *Wetlands*, *44*(8), 117.
22. Thomas, B. F., Behrangi, A., & Famiglietti, J. S. (2016). Precipitation intensity effects on groundwater recharge in the southwestern United States. *Water*, *8*(3), 90.
23. Veeranna, J., & Jeet, P. (2021). Management: A Case Study. *Groundwater Management and Resources*, 37.

24. Westenbroek, S. M., Engott, J. A., Kelson, V. A., & Hunt, R. J. (2018). *SWB Version 2.0--A Soil-Water-Balance Code for Estimating Net Infiltration and Other Water-Budget Components* (pp. 118-118). US Department of the Interior, US Geological Survey.
25. Wilson, K. B., Hanson, P. J., Mulholland, P. J., Baldocchi, D. D., & Wullschleger, S. D. (2001). A comparison of methods for determining forest evapotranspiration and its components: sap-flow, soil water budget, eddy covariance and catchment water balance. *Agricultural and forest Meteorology*, *106*(2), 153-168.
26. Yoon, J., Yi, S., Lee, E., Ji, J., Lee, S., & Yi, J. (2025). Assessing the Impact of Hydropower to Multipurpose Dam Reoperation on Downstream Hydrology and Water Quality. *Water*, *17*(22), 3191.
27. U.S. Department of Agriculture, Soil Conservation Service. (1986). *Urban hydrology for small watersheds* (Technical Release No. 55, 2nd ed.). U.S. Department of Agriculture.
28. U.S. Department of Agriculture, Natural Resources Conservation Service. (1997). *National engineering handbook: Section 4—Hydrology (Part 630).*